East European Journal of Physics. **4.** 298-307 (2025)
DOI:10.26565/2312-4334-2025-4-28 ISSN 2312-4334

ENERGY TRANSPORT IN A MHD HYBRID NANOFLUID FLOW OVER A POROUS EXPONENTIALLY STRETCHING SHEET

Mahesh Joshi[§], G. Venkata Ramana Reddy*
Department of Mathematics, Koneru Lakshmaiah Education Foundation,
Green fields, Vaddeswaram, Guntur-522302, Andhra Pradesh, India
**Corresponding Author: gvrr1976@kluniversity.in, [§]E-mail: mjprince939@gmail.com*
Received August 3, 2025; revised September 15, 2025; in final form September 17, 2025; accepted September 22, 2025

This study presents an in-depth analysis of the heat transfer mechanisms and fluid flow behavior associated with hybrid nanofluids in the presence of an exponentially stretching surface. Hybrid nanofluids, formed by dispersing more than one type of nanoparticle within a base fluid, exhibit superior thermophysical properties compared to conventional nanofluids. Their enhanced thermal conductivity, modified density, and tailored specific heat capacity make them highly suitable for advanced applications in nanotechnology, renewable energy systems, high-performance electronics cooling, and industrial-scale heat exchangers. The novelty of the present research lies in its attempt to explore the combined impact of hybrid nanoparticles and exponential stretching on boundary layer dynamics, thereby offering new insights into optimizing thermal systems. The core aim of this investigation is to maximize heat transfer efficiency under varying physical and operational conditions. To achieve this, the governing partial differential equations describing the conservation of mass, momentum, and energy are transformed into a set of nonlinear ordinary differential equations using similarity transformations and appropriate dimensionless parameters. This mathematical reformulation simplifies the complexity of the problem while preserving the essential physics of the flow. A computational framework is developed in MATLAB, where the coupled system of equations is solved using the fourth-order Runge–Kutta method integrated with a shooting technique to ensure accuracy and stability. The analysis highlights the roles of key parameters such as magnetic field intensity, Eckert number (viscous dissipation effects), Prandtl number (thermal diffusivity effects), and thermal radiation on velocity profiles, temperature distributions, and porous medium behavior. The results not only reveal the sensitivity of the flow and thermal fields to these controlling factors but also identify regimes where hybrid nanofluids significantly outperform traditional working fluids.
Keywords: *Lorentz force; Dissipation; Magneto-hydro dynamics (MHD); Hybrid nanofluids; Exponential stretching sheet*
PACS: 41.20.-q, 47.10.-g, 52.30.Cv, 47.10.A-, 47.65.-d

Nomenclature

Notation	Definition	Units	Notation	Definition	Units
u_1, u_2	Velocity profiles along x, y directions	-	Ec	Eckert number	-
U , V	Exponential rate and Velocity rate	-	Nu	Nusselt number	-
μ	Dynamic viscosity	[M L^{-1} T^{-1}]	Pr	Prandtl number	-
ρ	Fluid density	[M^{1}L^{-3}T^0]	K	Porosity parameter	-
η	Dimensionless distance	-	B_0	Magnetic field strength	[L^{-1}A]
M	Magnetic parameter	[M T^{-2} I^{-1}]	q_r	Radiative heat flux	[W/m^2]
Q	Heat source	[J/s] or [W]	β	Thermal expansion	[K^{-1}]
Cp	Specific heat	[M^{0}L^{2}T^{-2}K^{-1}]	ν	Kinematic viscosity	[M L^{-1} T^{-1}]
α	Thermal diffusivity	[L^{2}T^{-1}]	l	Length	[m]
σ	Electrical conductivity	[M^{-1}L^{-3}T^{3}A^2]	ϕ	Volume fraction	-
T	Temperature	[K]	ρCp	Heat Capacitance	[ML^{2}T^{-2}K^{-1}]
T_w	Wall stream temperature	[K]	c_0	Positive constant	-
T_∞	Free stream temperature	[K]	C_f	Skin friction	-
k	Thermal conductivity	[MLT^{-3}K^{-1}]	Re	Reynolds number	-
R	Radiation parameter	-	S	Suction parameter	-

INTRODUCTION

A fluid is a substance that encompasses both liquids and gases, characterized by its ability to deform and flow continuously when subjected to external forces such as pressure or shear stress. Unlike solids, fluids cannot resist shear stress and instead redistribute themselves until equilibrium is achieved. They exhibit key physical properties such as density, viscosity, temperature, and pressure, which determine their behavior under different flow conditions. The scientific study that deals with the motion and interaction of fluids is known as Fluid Dynamics, a core branch of Fluid Mechanics, which plays a vital role in understanding and predicting phenomena like turbulence, drag, lift, and flow stability. Such knowledge is crucial in applications ranging from aerodynamics and hydrodynamics to biomedical flows

Cite as: M. Joshi, G.V.R. Reddy, East Eur. J. Phys. 4, 298 (2025), https://doi.org/10.26565/2312-4334-2025-4-28

and industrial processes. Recent advancements in this field include the incorporation of nanoparticles into conventional base fluids like water, ethylene glycol, or engine oil, creating nanofluids with enhanced thermal and flow characteristics. Heat transfer, a fundamental aspect of fluid flow, involves the exchange of energy driven by temperature differences and occurs mainly through conduction, convection, and radiation. In fluids, convection becomes particularly significant as the bulk motion of fluid particles aids in transferring thermal energy efficiently, making fluid dynamics essential for designing advanced cooling, heating, and energy conversion systems. Choi [1], one who initiated the concept of nanoparticles, which can incorporate into the base fluids to generate a nanofluid. The size of a nanoparticle varies anyplace between 1-100 nm. Nanofluids imparts better properties, primarily thermal conductivity, also gives the abundant impact on velocity, temperature profiles. Nanofluids have a rich amount of research conducted within the last decades comprising preparation, characterization, modelling, convective, boiled heat transfer, and their applications [2-4].

A mixture of two nanoparticles into single base fluid is indicated as Hybrid nanofluids. Suresh [5] first proposed the theory of hybrid nanofluids to rise the valuable factors of normal nanomaterials. On extending more than two nanoparticles, consists the properties of thermophysical and chemical which lift the intensity in heat transfer [6]. Hybrid nanofluids come out with a promising result to enhance the attainment of heat transfer compared to traditional fluids and nanofluids with single nanoparticle [7]. There will be a high significant rate of thermal conductivity on applying two different nanoparticles to the fluid facilitating heat transfer [8]. Implementing two nanoparticles in the base fluid leads in prevention of particle sedimentation that ensures continuing stability of nanofluid and better their dispersion in the base fluid which can improve the heat transfer [9]. When the magnetic field is assigned in the hybrid nanofluid, Lorentz force acts on the particles that are charged inside the fluid heading to discrete effects and reactions. It exerts the substantial reference in the performance of hybrid nanofluids [10]. To make the transformation of heat strengthen, the flow patterns in the hybrid nanofluids are manipulated by managing the magnetic field [11]. Lorentz force helps in nanoparticle dispersion to make thermal conductivity and heat transfer more efficient [12]. During the flow of fluid, the K.E converts to thermal energy, this effects the friction behaviour of hybrid nanofluids and leads to viscous dissipation [13]. In enhancing the heat transfer rates, an increase in the fluid temperature is due to dissipation criteria [14]. The heat created from dissipation can alter the patterns of flow, changes in velocity profiles, and boundary layer thickness [15]. Thermal radiation, a form of heat transfer that includes the emission of electromagnetic waves, impact the thermal behaviour of fluid, mainly when combined with nanoparticles [16]. On adding excess heat source to the fluid, induces to a thicker thermal boundary layer, that increases the heat transfer [17]. Lorentz force, Viscous dissipation, Thermal radiation effects collectively considered to provide an absolute nanofluid behaviour [18]. The stretching surface along the flow is very much important and utilizes in spin forming, rolling, wire gathering, cultivating crystal, and production of fibre glass, plastic, rubber and more. Stretching sheet, a surface that moves continuously, immersed in a fluid, it produces a boundary layer flow. Stretching rate, properties of fluid, nanoparticle concentration are the points in which the thickness of boundary layer is depended [19]. The velocity gradients in the boundary layer are controlled by the stretching rate. The higher stretching rate results in high velocity gradient around the surface [20]. Magyari and Keller [21] were the first to pose the implementation of exponential stretching sheet to explore the circulation of wall temperature and heat transfer characteristics. Detailed explanation in boundary layer flow of MHD over an exponential stretching sheet on regarding thermal radiation was developed by Mabood [22]. The latest study on the influence of nanoparticles along the flow and heat transference through exponential shrinking sheet, gave the enhanced thermal boundary layer thickness as volume fraction of nanoparticle increased because of shrinking sheet [23].

Here, in this study the consideration of Lorentz force, thermal radiation, viscous dissipation are interacted to better the nanofluid nature. This combination will impact heat variation and flow features mainly in the plot involving magnetic fields and raised temperatures. Exploring all closely might provide a exact representation of nanofluid development [24]. Several outcomes are reported in the above literature, which are not reported to the whole. Accordingly, the main intention is to enquire the heat transfer and behaviour of fluid flow of Hybrid nanofluids forward to exponential stretching sheet with the Copper (Cu) and Titanium dioxide (TiO_2) as nanoparticles merged in the Water (H_2O) which is a base fluid. This appeal brings a novel perspective on shaping various forces that acts along the fluid flow. The results are shown both in tabulated and graphical form to the close extent compared to the previous works and conclusions are also clearly drafted.

MATHEMATICAL MODEL

Let us consider a two-dimensional hybrid nanofluid flow that is independent of time, with Titanium dioxide (TiO_2) and Copper (Cu) as nanoparticles, and Water (H2O) as the base fluid, to examine on an exponential stretching sheet. The x-axis is parallel and the y-axis is perpendicular to the surface, respectively (Fig. 1). The sheet elongates along the x-direction at an exponential rate of $U = c_0 e^{x/l}$ and the velocity profile as $V = c_0 e^{x/2l}$ (where l is length and c_0 is the positive stretching constant). The sheet is placed at an exponentially varying temperature $T_w = T_\infty + T_0 e^{x/2l}$ (where T_0, T_∞ are the reference value and the ambient value, respectively.

The vector notations for the fluid flow are

$$\nabla . u = 0 \tag{1}$$

The above represents the vector form of equation of continuity that expresses the law of conservation of mass for incompressible fluids.

$$(u.\nabla)u=\nu\nabla^2u_1-\frac{\sigma_{hnf}}{\rho_{hnf}}B_0^2(x)u_1-\frac{\mu_{hnf}}{\rho_{hnf}}\frac{u_1}{K} \tag{2}$$

This equation is essentially the Navier-Stokes momentum equation for a hybrid nanofluid that flows through the porous medium under a magnetic field. The vector form unifies the inertia, viscous, magnetic, and porous drag.

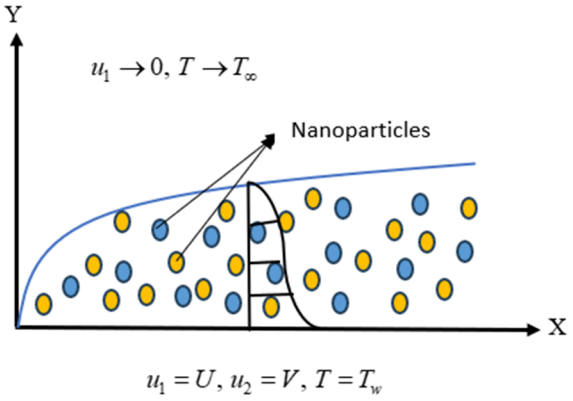

Figure 1. Model of the problem

$$(u.\nabla)T=\alpha_{hnf}\nabla^2T-\frac{1}{(\rho Cp)_{hnf}}\nabla q_r+\frac{Q}{(\rho Cp)_{hnf}}(T-T_\infty)+\frac{\mu_{hnf}}{(\rho Cp)_{hnf}}\Phi \tag{3}$$

The above is the energy equation along a porous path for hybrid nanofluids with heat source, viscous dissipation, and radiative heat flux in vector form.

The governing equations that were modified from the vector form are [25,26].

Continuity equation:

This is the mathematical expression of conservation of mass in an incompressible fluid flow.

$$\frac{\partial u_1}{\partial x}+\frac{\partial u_2}{\partial y}=0 \tag{4}$$

Momentum equation:

Equation (4) undergoes the principle of Newton's second law, where the change in momentum is directly proportional to the net forces acting on it and represents the convection flow change on the left side and viscous effects, magnetic forces, thermal conductivity respectively to the right of the equation.

$$u_1\frac{\partial u_1}{\partial x}+u_2\frac{\partial u_1}{\partial y}=\left(\frac{\mu_{hnf}}{\rho_{hnf}}\right)\frac{\partial^2u_1}{\partial y^2}-\left(\frac{\sigma_{hnf}}{\rho_{hnf}}\right)B_0^2(x)u_1-\left(\frac{\mu_{hnf}}{\rho_{hnf}}\right)\frac{u_1}{K} \tag{5}$$

Energy equation:

The change in total energy is equal to the summation of the rate of work done by force applied and change in heat quantity per unit time. The equation below describes the change of convection flow to the left and thermal diffusion, radiative heat flux gradient, heat generation with temperature differences, and viscous dissipation to the right accordingly in the equation.

$$u_1\frac{\partial T}{\partial x}+u_2\frac{\partial T}{\partial y}=\alpha_{hnf}\frac{\partial^2T}{\partial y^2}-\frac{1}{(\rho Cp)_{hnf}}\frac{\partial q_r}{\partial y}+\frac{Q}{(\rho Cp)_{hnf}}(T-T_\infty)+\frac{\mu_{hnf}}{(\rho Cp)_{hnf}}\left(\frac{\partial u_1}{\partial y}\right)^2 \tag{6}$$

Radiative heat flux qr is possible to write by taking advantage of Rosseland approximation as [25]

$$q_r=-\frac{4\sigma^*}{3k^*}\left(\frac{\partial T^4}{\partial y}\right) \tag{7}$$

σ^* is the Stephen Boltzmann constant and k^* is the absorption coefficient

$$T^4\cong 4T_\infty^3T-3T_\infty^4 \tag{8}$$

Incorporating the value of T^4 in the equation (7) we obtain

$$q_r = -\frac{16\sigma^* T_\infty^3}{3k^*}\left(\frac{\partial T}{\partial y}\right) \tag{9}$$

Equation (6) takes the form after including the Rosseland approximation q_r of equation (8)

$$u_1\frac{\partial T}{\partial x}+u_2\frac{\partial T}{\partial y}=\alpha_{hnf}\frac{\partial^2 T}{\partial y^2}+\frac{16\sigma^* T_\infty^3}{(\rho Cp)_{hnf}\,3k_1}\frac{\partial^2 T}{\partial y^2}+\frac{Q}{(\rho Cp)_{hnf}}(T-T_\infty)+\frac{\mu_{hnf}}{(\rho Cp)_{hnf}}\left(\frac{\partial u_1}{\partial y}\right)^2 \tag{10}$$

Boundary conditions are

$$\begin{aligned} &u_1 = U,\ \ u_2 = V,\ \ T = T_w,\ \ at\ \ y \to 0 \\ &u_1 \to 0,\ \ T \to T_\infty,\ \ as\ \ y \to \infty \end{aligned} \tag{11}$$

Considered similarity transformations are [26,28]

$$\begin{aligned} &\eta = y\sqrt{\frac{c_0}{2\nu l}}e^{\frac{x}{2l}},\ u_1 = c_0 e^{\frac{x}{l}} f'(\eta),\ u_2 = -\sqrt{\frac{c_0\nu}{2l}}e^{\frac{x}{2l}}\left[f(\eta)+\eta f'(\eta)\right], \\ &T = T_\infty + T_0 e^{\frac{x}{2l}}\theta(\eta) \end{aligned} \tag{12}$$

Using relations of equation (8), equation (4) is satisfied and equation (5) & (6) respectively converted to

$$f''' - a_1 a_3 M f' - 2a_1 a_2 f'^2 - Kf' + a_1 a_2 f f'' = 0 \tag{13}$$

$$a_1\left(a_5+\frac{4}{3}R\right)\theta'' + a_1 a_4 \,\mathrm{Pr}\, f\theta' - a_1 a_4 \,\mathrm{Pr}\, f'\theta + a_1 \,\mathrm{Pr}\,\beta\theta + \mathrm{Pr}\, Ecf''^2 = 0 \tag{14}$$

Boundary conditions are transferred to,

$$\begin{aligned} &f'(0) = 1,\ f(0) = S,\ \theta(0) = 1,\ \ at\ \eta = 0 \\ &f'(\infty) \to 0,\ \theta(\infty) \to 0,\ as\ \ \eta \to \infty \end{aligned} \tag{15}$$

The dimensionless parameters are

$$M = \frac{2\sigma_f B_0^2 l}{(Cp)_f},\ \mathrm{Pr} = \frac{\mu_f (Cp)_f}{k_f},\ Ec = \frac{U_w^2}{(Cp)_f (T_w - T_\infty)},$$

$$R = \frac{4\sigma^* T_\infty^3}{k^* k_f},\ K = \frac{2l\nu_f}{c_0 \mathrm{K}_0},\ \beta = \frac{2lQ_0}{c_0 (\rho Cp)_f},\ S = -c_0\sqrt{\frac{2l}{\nu_f c_0}}$$

where M is the magnetic parameter, R is the radiation parameter, Pr is the Prandtl number, Ec is the Eckert number, β represents the thermal expansion, s is the suction parameter and K is the porosity parameter.

Quantities of engineering: Physical quantities known as skin friction and Nusselt number are mentioned as follows:

$$C_{fx} - \frac{\mu_{hnf}}{\rho_f U^2}\left(\frac{\partial u_1}{\partial y}\right)_{y=o} = 0$$

$$Nu_x + \frac{2l}{k_f (T_w - T_\infty)}\left(-k_{hnf}\left(\frac{\partial T}{\partial y}\right)_{y=o} + (q_r)_{y=0}\right) = 0$$

The dimensionless forms of Skin friction and Nusselt number

$$Cf_x\,\mathrm{Re}_x^{\frac{1}{2}} = \left(\frac{f''(0)}{a_1}\right),\ Nu_x\,\mathrm{Re}_x^{\frac{-1}{2}} = -\left(a_4 + \tfrac{4}{3}R\right)\theta'(0)$$

Table 1. Thermophysical models for Hybrid nanofluids [26]

Properties	Hybrid nanofluid
Viscosity	$a_1 = \frac{\mu_{hnf}}{\mu_f} = (1-\phi_1)^{2.5}(1-\phi_2)^{2.5}$
Density	$a_2 = \frac{\rho_{hnf}}{\rho_f} = (1-\phi_2)\left[1-\phi_1+\phi_1\left(\frac{\rho_1}{\rho_f}\right)\right]+\phi_2\left(\frac{\rho_2}{\rho_f}\right)$
Electrical conductivity	$a_3 = \frac{\sigma_{hnf}}{\sigma_f} = 1+\frac{3\left(\frac{\phi_1\sigma_1+\phi_2\sigma_2}{\sigma_f}-(\phi_1-\phi_2)\right)}{2+\left(\frac{\phi_1\sigma_1+\phi_2\sigma_2}{\sigma_f(\phi_1+\phi_2)}\right)-\left(\frac{\phi_1\sigma_1+\phi_2\sigma_2}{\sigma_f}-(\phi_1+\phi_2)\right)}$
Specific heat	$a_4 = \frac{(\rho Cp)_{hnf}}{(\rho Cp)_f} = (1-\phi_2)\left[1-\phi_1+\phi_1\left(\frac{(\rho Cp)_1}{(\rho Cp)_f}\right)\right]+\phi_2\left(\frac{(\rho Cp)_2}{(\rho Cp)_f}\right)$
Thermal conductivity	$a_5 = \frac{k_{hnf}}{k_f} = \frac{k_2+2k_{nf}-2\phi_2(k_{nf}-k_2)}{k_2+2k_{nf}+2\phi_2(k_{nf}-k_2)}$, $at\ k_{nf} = \frac{k_1+2k_{nf}-2\phi_1(k_{nf}-k_1)}{k_1+2k_{nf}+2\phi_1(k_{nf}-k_1)}\times k_f$

Table 2. Thermal properties of Water, nanoparticles [26]

Property	Cu	TiO_2	H_2O
Density 'ρ' (kg/m^3)	8933	4250	997.1
Specific heat 'Cp' (J/kg-K)	385	686.2	4179
Thermal conductivity 'k' (W/m-K)	400	8.9538	0.613
Electrical conductivity 'σ' (S/m)	5.96×10^7	2.38×10^6	5×10^{-2}

Methodology

This flowchart outlines the computational procedure for solving a boundary value problem (BVP) using MATLAB's bvp4c solver. It begins with variable declaration and initialization, followed by domain quantization to discretize the problem space. The core process starts by calling bvp4c, which requires defining a system of first-order ordinary differential equations (ODEs) and appropriate boundary conditions. Boundary conditions are either exactly known for the first solution or initially guessed for subsequent solutions. The process iteratively adjusts these guesses to match desired solutions, such as the second, third, or fourth, refining them to improve accuracy. Once the boundary conditions are properly set and the function is evaluated, the solver computes the numerical results, yielding the final solution of the BVP.

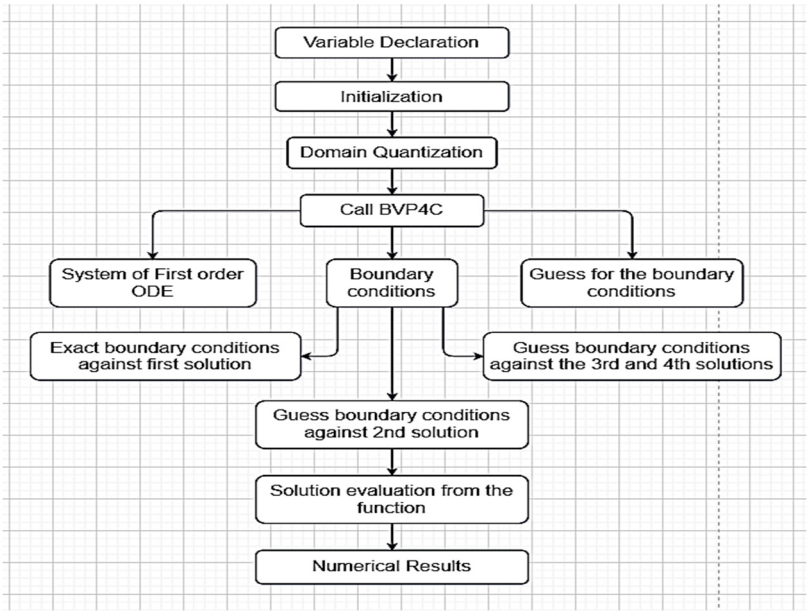

Figure 2. Flowchart of numerical solution

The system of Ordinary differential equations derived from equations (13) & (14), along with their respective boundary conditions given in equation (15), is solved numerically using the shooting method. To convert those equations into a first-order ODE, we initiate the variables as

$$f = f(1), f' = f(2), f'' = f(3), \theta = f(4), \theta' = f(5)$$

$$f''' = a_1 a_3 M f(2) + 2a_1 a_2 \left(f(2)^2 \right) + K f(2) - a_1 a_2 f f(3)$$

$$\theta = f(5)$$

$$\theta'' = \frac{a_1 a_4 \Pr f(2) f(4) - a_1 \Pr \beta f(4) - \Pr Ec \left(f(2)^2 \right) - a_1 a_4 \Pr f(1) f(5)}{a_1 \left(a_5 + \frac{4}{3} R \right)}$$

The corresponding dimensionless boundary conditions are

$$f(1) = S,\ f(2) = 1,\ f(4) = 1 \text{ at } \eta \to 0$$

$$f(2) \to 0,\ f(4) \to 0 \text{ at } \eta \to \infty$$

RESULTS AND DISCUSSION

The non-linear differential equations are solved using Runge-Kutta method under boundary conditions lead to numerous changes in the velocity, temperature profiles and in the effects of skin friction and Nusselt number are represented in graphical and tabular forms.

Table 3. Comparison of $-\theta'(0)$ with dissimilar values of *R, M, Pr*

R	M	Pr	Ishak et al. [27]	Goud et al. [28]	Present work
0	0	1.0	0.9548	0.9547	0.9540
0	0	2.0	1.4715	1.4714	1.4573
0	0	3.0	1.8691	1.8690	1.7893
0	0	5.0	2.5001	2.5001	2.3195
0	0	10.0	3.6603	3.6603	3.2694

Table 4. Mutations of $Cf_x \operatorname{Re}_x^{\frac{1}{2}}$ by Pr = 6.2; R = 1.0; Ec = 0.3; $\beta = 0.1$

M	K	s	ϕ_1	ϕ_2	Zahid et al. [25]	Present work
0.5	1.0	0.1	0.1	0.1	-3.2211	-2.8553
1.0	1.0	0.1	0.1	0.1	-3.3551	-3.1546
1.5	1.0	0.1	0.1	0.1	-3.4836	-3.4277
2.0	1.0	0.1	0.1	0.1	-3.6073	-3.6805

Table 5. Changes of $Nu_x \operatorname{Re}_x^{\frac{-1}{2}}$ by Pr = 6.2; K = 1.0; s = 0.1

M	Ec	R	β	ϕ_1	ϕ_2	Zahid et al. [25]	Present work
0.5	0.3	1.0	0.1	0.1	0.1	1.3487	1.3480
1.0	0.3	1.0	0.1	0.1	0.1	1.1466	1.1465
1.5	0.3	1.0	0.1	0.1	0.1	0.9518	0.9510
2.0	0.3	1.0	0.1	0.1	0.1	0.7570	0.7572

As the magnetic parameter increases, the Lorentz force intensifies, leading to a reduction in the fluid's drift velocity. When a magnetic field is applied to a fluid, it induces a resistive force known as the Lorentz force, which acts against the fluid's motion. Thus, the velocity is decreased in Figure 3.

From Figure 4 the temperature is raised on increasing the magnetic parameter due to the interaction between electrically conducting fluid and the magnetic field, called Lorentz force, generates the friction within the fluid converting the kinetic energy to thermal energy causes the temperature increment.

Figure (5), represents the increment in the porosity parameter leads to increase in the velocity, because a higher porosity means there are more interconnected void spaces allowing the fluid to flow easily with less resistance.

In Figure 6 it is observed that temperature is increased on increase in the porosity parameter, this is noticed mainly in the context of porous medium because higher porosity allows for greater penetration and an increased surface area for heat transport.

Figure 7 shows the impact of the velocity profile on increasing the suction parameter, particularly at the boundary layer. This is because suction effectively removes fluid from the boundary layer, reducing the momentum of the flow and repeatedly slowing it down.

Figure 8 elaborates the decrease in temperature with an increase in the suction parameter, due to a better cooling effect from the increased fluid being drawn into the boundary layer. This effect helps in removing the heat effectively, resulting in the temperature reduction.

Figure 9 depicts the variations in the temperature by increasing the radiation parameter, this is because the fluid is absorbing its own thermal radiation and increase heat transfer from heat surfaces. This showed the increase in the temperature on increasing in the radiation parameter.

Figure 10 shows the increase in the temperature while the values of Eckert number are increased. As Eckert number increases, the viscous dissipation in the fluid becomes more significant, which converts the kinetic energy to thermal energy, that results in the temperature increment.

Figures (11) & (12), separately shows the representation of variations in temperature profile on increasing the volume fractions of Copper and Titanium dioxide nanoparticles respectively. This result in the increase of temperature because increase in the particles can increase the surface areas for heat exchanging also can absorb excess heat leading to the high temperatures.

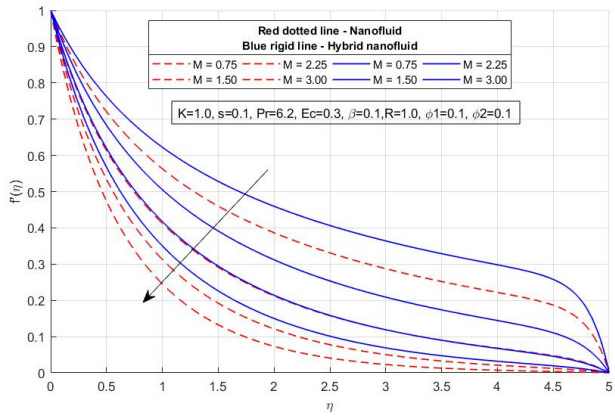

Figure 3. Difference in velocity profile for various values of M

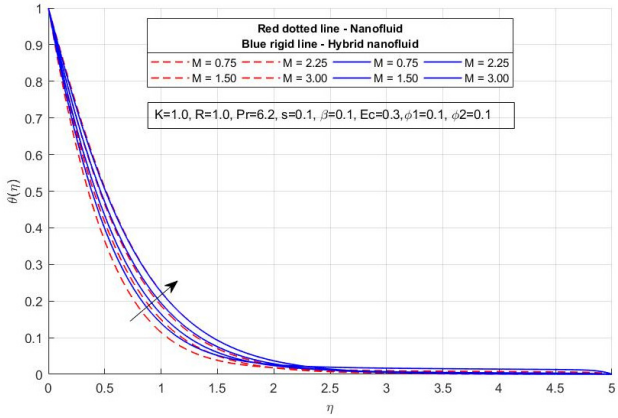

Figure 4. Variations of temperature profile for distinct values of M

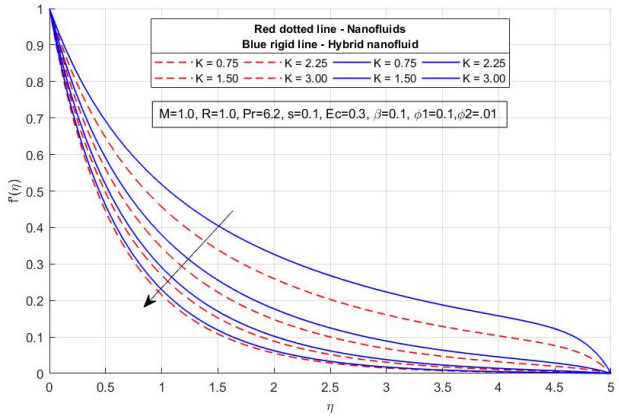

Figure 5. Difference in velocity profile with distinct values of K

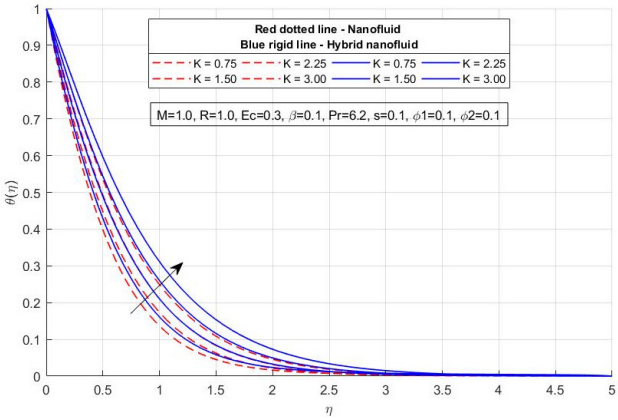

Figure 6. Variations in temperature profile for distinct values of K

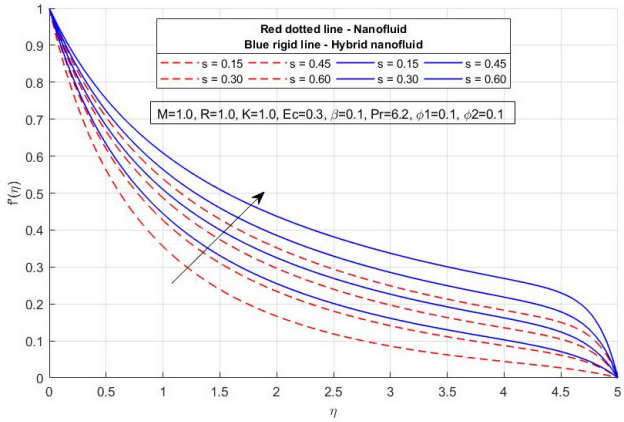

Figure 7. Difference in velocity profile for distinct values of s

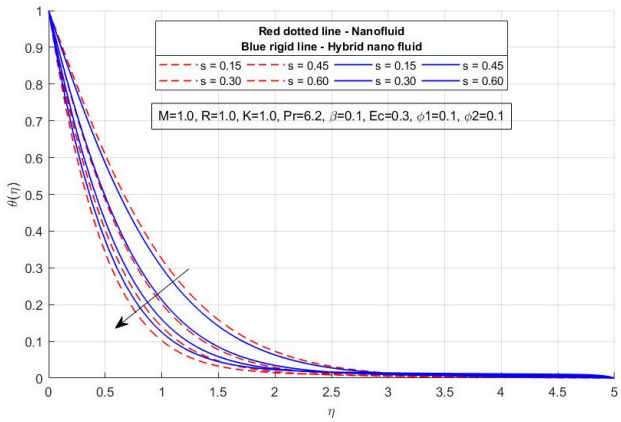

Figure 8. Variations in temperature profile for different values of s

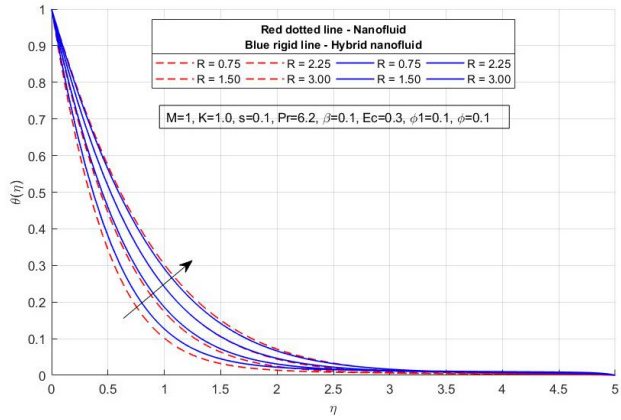

Figure 9. Variances in temperature profile with distinct values of R

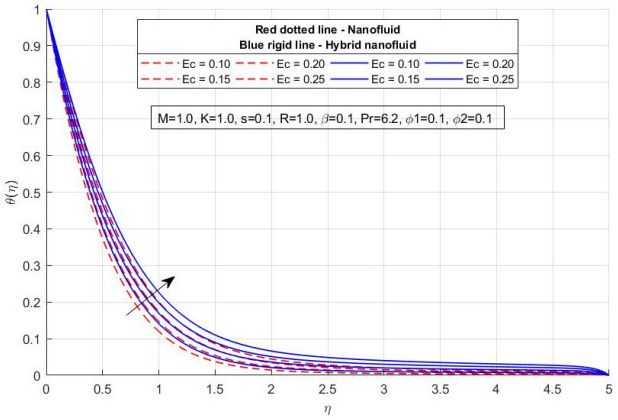

Figure 10. Variances of temperature profile with distinct values of Ec

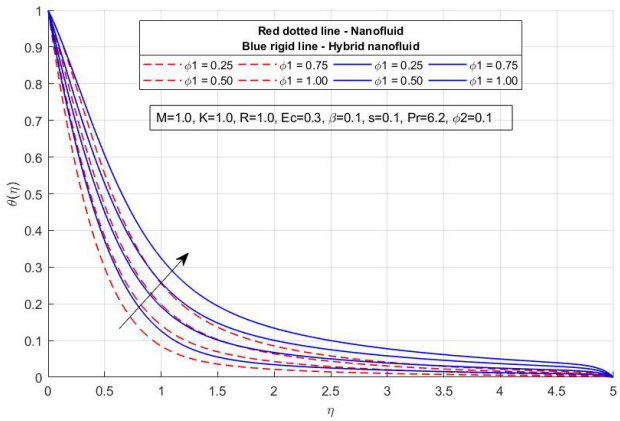

Figure 11. Variances of temperature profile for distinct values of ϕ_1

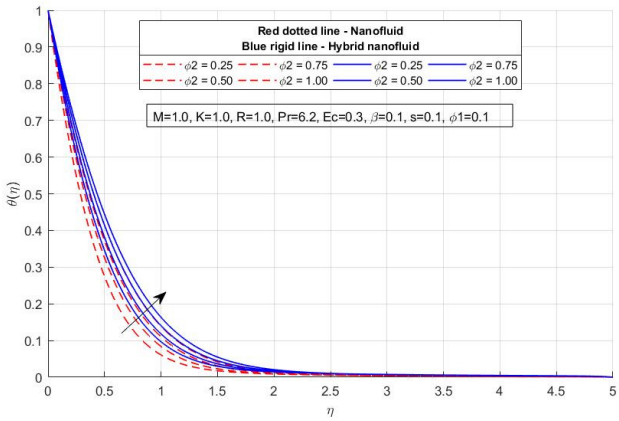

Figure 12. Variances in temperature profiles for distinct values of ϕ_2

CONCLUSIONS

The outcomes of this research establish that the synergistic effect of hybrid nanoparticles and exponential surface stretching significantly advances heat transfer performance while offering deeper insights into boundary layer control. By integrating magnetohydrodynamic influences, viscous dissipation, and radiative effects, the study not only enhances the predictive accuracy of nanofluid-based thermal models but also identifies optimal operating conditions for engineering applications. These findings contribute novel perspectives toward the design of next-generation thermal management systems, particularly in energy, electronics, and advanced manufacturing sectors, where precise regulation of heat transfer is essential. A broad range of investigation is done on the Hybrid nanofluid flow and heat transfer which included two nanoparticles namely Titanium dioxide (TiO_2) and Copper (Cu) and the base fluid used is Water (H_2O) on exponential stretching sheet. To validate, the present results are compared with the previously published articles, achieved good outcomes. On inclusion of the different parameters on the fluid velocity and temperature profiles were solved by attaining Runge-Kutta method of Shooting technique. The important disclosures are generalised here:

- The velocity component is decreased slightly on productivity of Magnetic parameter, Porosity parameter, Suction parameter.
- On increasing the Magnetic parameter, Porosity parameter there is an increase in the temperature profile in the both mentioned parameters.
- The values of temperature profiles and volume fractions are seen in proportional on increasing in the volume fractions.
- The magnetic parameter, suction parameter, porosity parameter are conversely related to the drag co-efficient of the volume fractions.
- By improving the suction parameter values there is an adequate downfall of velocity profile and temperature profile.
- The Radiation parameter consumes a productive association with rate of heat transfer whereas the magnetic parameter, viscous dissipation parameter, volume fractions of the nanoparticles all possess negative correlation.

In the coming research, the above work could be extended by engaging novel fluids and appropriate effects like space dependent heat sources.

ORCID

Mahesh Joshi, https://orcid.org/0009-0005-7486-2361; **G. Venkata Ramana Reddy,** https://orcid.org/0000-0002-6455-3750

REFERENCES

[1] S.U. Choi, and J.A. Eastman, *Enhancing thermal conductivity of fluids with nanoparticles* (No. ANL/MSD/CP-84938; CONF-951135-29). Argonne National Lab. (ANL), Argonne, IL (United States, 1995).

[2] J. Sarkar, "A critical review of heat transfer correlations of nanofluids," Renew Sustain Energy Rev. **15**, 3271–3277 (2011). https://doi.org/10.1016/j.rser.2011.04.025

[3] W. Yu, and H. Xie, "A review on nanofluids: preparation, stability mechanisms, and applications," J. Nano mater. **2012**, 435873 (2012). https://doi.org/10.1155/2012/435873

[4] K.V. Wong, and O.D. Leon, "Applications of nanofluids: current and future," Adv. Mech. Eng. **2010**, 519659 (2010). https://doi.org/10.1155/2010/519659

[5] S. Suresh, K. Venkitaraj, P. Selvakumar, and M. Chandrasekar, "Experimental investigation of mixed convection with synthesis of Al2O3 using two step method and its thermophysical properties," Colloid. Surface. **8**, 41–48 (2011). https://doi.org/10.1016/j.colsurfa.2011.08.005

[6] J. Sarkar, P. Ghosh, and A. Adil, "A review on hybrid nanofluids: recent research, development, and applications," Renew. Sustain. Energy Rev. **43**, 164–177 (2015). https://doi.org/10.1016/j.rser.2014.11.023

[7] I. Waini, A. Ishak, and I. Pop, "Unsteady flow and heat transfer past a stretching/shrinking sheet in a hybrid nanofluid," International Journal of Heat and Mass Transfer, **136**, 288-297 (2019). https://doi.org/10.1016/j.ijheatmasstransfer.2019.02.101

[8] B. Yashkun, *et al*., "Effect of thermal radiation and suction on MHD hybrid nanofluid flow and heat transfer over a stretching/shrinking sheet," Journal of Molecular Liquids, **315**, 113800 (2020).

[9] G. Tharapatla, V.L. Garishe, N. Vijaya, S. Wuriti, and G.V.R. Reddy. "MHD Hybrid Nanofluids Flow Through Porous Stretching Surface in the Presence of Thermal Radiation and Chemical Reaction," East European Journal of Physics, (3) 158-167 (2025). https://doi.org/10.26565/2312-4334-2025-3-14

[10] M. Sheikholeslami, S. Zahir, S. Ahmad, K. Poom, and H. Babazadeh, "Lorentz force impact on hybrid nanofluid within a porous tank including entropy generation", International Communications in Heat and Mass Transfer, **116**, 104635 (2020). https://doi.org/10.1016/j.icheatmasstransfer.2020.104635

[11] S.S.U. Devi, and S.A. Devi, "Numerical investigation of three-dimensional hybrid Cu-Al2O3/water nanofluid flow over a stretching sheet with effecting Lorentz force subject to Newtonian heating," Can. J. Phys. **94**, 490–496 (2016). https://doi.org/10.1139/cjp-2015-0799

[12] D. Yadav, J. Wang, J. Lee, and H.H. Cho, "Numerical investigation of the effect of magnetic field on the onset of nanofluid convection," Appl. Ther. Eng. **103**, 1441–1449 (2016). https://doi.org/10.1016/j.applthermaleng.2016.05.039

[13] R. Cortell, "Effects of viscous dissipation and radiation on the thermal boundary layer over a nonlinearly stretching sheet," Phys. Lett. A, **372**, 631–636 (2008). https://doi.org/10.1016/j.physleta.2007.08.005

[14] A. Ali, A. Noreen, S. Saleem, A.F. Aljohani, and M. Awais, "Heat transfer analysis of Cu–Al2O3 hybrid nanofluid with heat flux and viscous dissipation," Journal of Thermal Analysis & Calorimetry, **143**(3), 2367 (2021). https://doi.org/10.1007/s10973-020-09910-6

[15] K.L. Hsiao, "Micropolar nanofluid flow with MHD and viscous dissipation effects towards a stretching sheet with multimedia feature," Int. J. Heat Mass Transf. **112**, 983–990 (2017). https://doi.org/10.1016/j.ijheatmasstransfer.2017.05.042

[16] N.A. Zainal, R. Nazar, K. Naganthran, and I. Pop, "The Impact of Thermal Radiation on Maxwell Hybrid Nanofluids in the Stagnation Region," Nanomaterials (Basel), **12**(7), 1109 (2022). https://doi.org/10.3390/nano12071109

[17] H. Waqas, U. Farooq, D. Liu, M. Abid, M. Imran, and T. Muhammad, "Heat transfer analysis of hybrid nanofluid flow with thermal radiation through a stretching sheet: A comparative study," Int. Commun. Heat Mass Transf. **138**, 106303 (2022). https://doi.org/10.1016/j.icheatmasstransfer.2022.106303

[18] T. Hayat, M.I. Khan, M. Waqas, A. Alsaedi, and M. Farooq, "Numerical simulation for melting heat transfer and radiation effects in stagnation point flow of carbon–water nanofluid," Comput. Methods Appl. Mech. Eng. **315**, 1011–1024 (2017). https://doi.org/10.1016/j.cma.2016.11.033

[19] W. Khan, and I. Pop, "Boundary-layer flow of a nanofluid past a stretching sheet," Int. J. Heat Mass Transf. **53**, 2477–2483 (2010). https://doi.org/10.1016/j.ijheatmasstransfer.2010.01.032

[20] N. Acharya, K. Das, K.P. Kumar, "Ramification of variable thickness on MHD TiO and Ag nanofluid flow over a slendering stretching sheet using NDM," Eur. Phys. J. Plus, **131**, 303 (2016). https://doi.org/10.1140/epip/i2016-16303-4

[21] E. Magyari, and B. Keller, "Heat, and mass transfer in the boundary layers on an exponentially stretching continuous surface," J. Phys. D Appl. Phys. **32**, 577 (1999). https://doi.org/10.1088/0022-3727/32/5/012

[22] F. Mabood, W. Khan, and A.M. Ismail, "MHD flow over exponential radiating stretching sheet using homotopy analysis method," J. King Saud Univ.-Eng. Sci. **29**, 68–74 (2017). https://doi.org/10.1016/j.jksues.2014.06.001

[23] A. Zaib, K. Bhattacharyya, and S. Shafie, "Unsteady boundary layer flow and heat transfer over an exponentially shrinking sheet with suction in a copper-water nanofluid," J. Cent. South Univ. **22**, 4856–4863 (2015). https://doi.org/10.1007/s11771-015-3037-1

[24] N.A. Haroun, S. Mondal, and P. Sibanda, "Hydromagnetic nanofluids flow through a porous medium with thermal radiation, chemical reaction and viscous dissipation using the spectral relaxation method," Int. J. Comput. Methods, **16**, 1840020 (2019). https://doi.org/10.1142/S0219876218400200

[25] S. Rosseland, *Astrophysics and Atomic Theoretical Foundations*, (Springer: Berlin/Heidelberg, Germany, 1931).

[26] M. Zahid, A. Basit, T. Ullah, B. Ali, and G. Liskiewicz, "Coupled Effects of Lorentz Force, Radiation, and Dissipation on the Dynamics of a Hybrid Nanofluid over an Exponential Stretching Sheet," Energies, **16**, 7452 (2023). https://doi.org/10.3390/en16217452
[27] I. Waini, A. Ishak, and I. Pop, "Hybrid nanofluid flow induced by an exponentially shrinking sheet," Chin. J. Phys. **68**, 468–482 (2020). https://doi.org/10.1016/j.cjph.2019.12.015
[28] A. Ishak, "MHD boundary layer flow due to an exponentially stretching sheet with radiation effect," Sains Malaysiana, **40**, 391-395 (2011). http://www.ukm.edu.my/jsm/pdf_files/SM-PDF-40-4-2011/17%20Anuar%20Ishak.pdf
[29] B.S. Goud, P. Srilatha, P. Bindu, and Y.H. Krishna, "Radiation effect on MHD boundary layer flow due to an exponentially stretching sheet," Adv. Math. Sci. J. **9**, 10755–10761 (2020). https://doi.org/10.37418/amsj.9.12.59

ЕНЕРГЕТИЧНИЙ ТРАНСПОРТ У ПОТОЦІ МГД-ГІБРИДНОЇ НАНОРІДИНИ НАД ПОРИСТИМ ЛИСТОМ З ЕКСПОНЕНЦІАЛЬНИМ РОЗТЯГНЕННЯМ

Махеш Джоші, Г. Венката Рамана Редді

Кафедра математики, Освітній фонд Конеру Лакшмаї, Зелені поля, Ваддесварам, Гунтур-522302, Андхра-Прадеш, Індія

Це дослідження представляє поглиблений аналіз механізмів теплопередачі та поведінки потоку рідини, пов'язаних з гібридними нанорідинами за наявності поверхні, що експоненціально розтягується. Гібридні нанорідини, утворені шляхом диспергування кількох типів наночастинок в базовій рідині, демонструють кращі теплофізичні властивості порівняно зі звичайними нанорідинами. Їхня підвищена теплопровідність, модифікована щільність та спеціалізована питома теплоємність роблять їх дуже придатними для передових застосувань у нанотехнологіях, системах відновлюваної енергії, високопродуктивному охолодженні електроніки та теплообмінниках промислового масштабу. Новизна цього дослідження полягає в його спробі дослідити комбінований вплив гібридних наночастинок та експоненціального розтягування на динаміку пограничного шару, тим самим пропонуючи нові ідеї щодо оптимізації теплових систем. Основною метою цього дослідження є максимізація ефективності теплопередачі за різних фізичних та експлуатаційних умов. Для досягнення цієї мети керівні диференціальні рівняння з частинними похідними, що описують закон збереження маси, імпульсу та енергії, перетворюються на набір нелінійних звичайних диференціальних рівнянь за допомогою перетворень подібності та відповідних безрозмірних параметрів. Таке математичне переформулювання спрощує складність задачі, зберігаючи при цьому основну фізику потоку. У MATLAB розроблено обчислювальну базу, де зв'язана система рівнянь розв'язується за допомогою методу Рунге-Кутти четвертого порядку, інтегрованого з методом стрільби для забезпечення точності та стабільності. Аналіз підкреслює роль ключових параметрів, таких як напруженість магнітного поля, число Екерта (ефекти в'язкої дисипації), число Прандтля (ефекти температуропровідності) та теплове випромінювання, на профілі швидкості, розподіл температури та поведінку пористого середовища. Результати не тільки показують чутливість потоку та теплових полів до цих контролюючих факторів, але й визначають режими, в яких гібридні нанорідини значно перевершують традиційні робочі рідини.

Ключові слова: *сила Лоренца; дисипація; магнітогідродинаміка (МГД); гібридні нанорідини; експоненціальне розтягування листа*